ELSEVIER

Journal of Biomechanics 35 (2002) 1019–1027

JOURNAL OF BIOMECHANICS

www.elsevier.com/locate/jbiomech
www.JBiomech.com

ASB post-doctoral young investigator award 2001

Tensile properties of in vivo human tendinous tissue

Constantinos N. Maganaris*

Centre for Biophysical and Clinical Research into Human Movement, Manchester Metropolitan University, Alsager ST7 2HL, UK

Accepted 8 March 2002

Abstract

The biomechanical properties of tendinous structures have traditionally been studied using excised material. Limitations associated with displacement measurements and clamping, and uncertainties as to whether in vitro testing represents physiological function, necessitate developing a method for assessing the mechanical properties of tendinous tissue in the in vivo state. This paper reviews recent results taken with an in vivo and noninvasive protocol using ultrasound as a means of measuring tendon-aponeurosis elongation during tensile loading applied by contraction of the in-series muscle. The results obtained indicate that: (1) the Young's modulus and mechanical hysteresis of in vivo tendons is independent of physiological function and loading, (2) there is a strain variation along the tendon-aponeurosis, and (3) in vivo tendons may exhibit creep. These findings agree with reports from experiments on isolated material and have important biological implications for both the tendon and the in-series muscle. The method described here allows designing longitudinal studies on tendon adaptability, but it also has direct clinical applications.

Keywords: Ultrasound; Tendon; Aponeurosis; Muscle; Contraction

1. Introduction

The primary role of tendons is to transmit contractile forces to the skeleton to generate joint movement. In doing so, however, tendons do not behave as rigid structures. They rather exhibit viscoelastic properties, which are important for the function of the muscle–tendon unit (for review see Alexander, 1988; Zajac, 1989). Most of these properties have been studied using excised animal tendons undergoing stretching imposed by the motor of a tensile-testing machine (for review see Viidik, 1973; Butler et al., 1978; Ker, 1992; Shadwick, 1992). However, several limitations inherent to isolated-material testing raise doubts as to whether results from excised tendons can be extrapolated directly to interpret in vivo physiological function:

(1) Stretching a clamped fibrous structure is inevitably associated with slippage of inner fibres and stress concentration in fibres adjacent to the clamp, resulting in larger elongations in the tendon regions near the clamps, negative Poison ratios, and premature failure (Ker, 1992; Shadwick, 1992). These problems can be circumvented by measuring tensile deformations over a restricted region away from the tendon-clamped ends, but such measurements may not represent the mechanical behaviour of the entire specimen (Zernicke et al., 1984).

(2) Many of the experiments in the literature have been performed using preserved or deep-frozen tendons, which may have altered properties (Matthews and Ellis, 1968; Smith et al., 1996).

(3) Tendon loads within the physiological region have traditionally been applied based on calculations incorporating the isometric stress-generating potential of the in-series muscle, which has been treated as a constant (Ker et al., 1988; Shadwick, 1990; Loren and Lieber, 1995; Pike et al., 2000). There is experimental evidence, however, that the maximal contractile isometric stress may differ between muscles, with fibre composition being the major determinant factor (Witzmann et al., 1983; Powell et al., 1984; Bottinelli et al., 1996).

A test avoiding the above problems could be a tensile test performed under in vivo conditions. In this paper, we review recent results produced using a novel method, which offers promise for realistic assessment of in vivo human tendon mechanical properties.

*Corresponding author. Tel.: +44-161-247-5428; fax: +44-161-247-6375.

E-mail address: c.n.maganaris@mmu.ac.uk (C.N. Maganaris).

0021-9290/02/$ - see front matter
PII: S0021-9290(02)00047-7

2. In vivo tendon mechanical properties

The method is based on in vivo quantification of the tendon load-elongation response. Tendon loads are generated by contraction of the in-series muscle, and the resultant tendon elongations are taken from ultrasound-based measurements of the displacement of an anatomical landmark in the tendon proximal end. To avoid displacements in the tendon bony attachment during contraction, the contractions are elicited with the limb secured at a fixed joint angle. The muscle moments generated by contraction can be quantified using a load cell, reduced to tendon forces using information about moment arm lengths, and then combined with the respective tendon elongations to obtain the tendon force-elongation relation.

We have applied the above principles to examine the mechanical behaviour of the human tibialis anterior (TA) and gastrocnemius (GS) tendons. These tendons were selected for a number of reasons: (1) They are superficial and therefore allow high-quality ultrasound scanning. (2) They are attached to muscles whose joint moments can be separated from those generated from other agonist and antagonist muscles. (3) Both tendons are important in locomotion.

Three series of experiments are presented in this paper. The first experiments were carried out to estimate the Young's modulus and the mechanical hysteresis of the two tendons (Maganaris and Paul, 1999, 2000a, 2002). These properties were examined with the ankle placed at the neutral anatomical position (the tibial axis at right angles to the sole of the foot) on the footplate of a dynamometer (Lido Active, Loredan Biomedical, Davis, USA). To obtain the mechanical properties of either tendon, the following four parameters were quantified: (1) the muscle's isometric moment-generating potential; (2) the tendon elongation during contraction–relaxation; (3) the tendon moment arm length; and (4) the tendon cross-sectional area and length at rest.

The experimental set-up is shown in Fig. 1. To isolate the mechanical action of the TA muscle, contractile forces were elicited by means of percutaneous, tetanic electrical stimulation (100 Hz for 2 s), using the maximal voltage that could be tolerated by the subject. EMG and ultrasound recordings were taken from nearby muscles to ensure the absence of current leakage during stimulation. To isolate the mechanical action of the GS muscle, we measured the net ankle moments generated during isometric plantarflexion maximal voluntary contractions (MVCs) with the knee fully extended (180°) and with the knee flexed at 60°, and we subtracted the MVC moment at the knee flexion position from that at the knee extension position. The resultant moment value was assumed to represent the moment-generating potential of the GS muscle (Herzog et al., 1990). The above calculation assumes that: (a) the GS muscle–tendon unit is slack at the knee flexion angle of 60° and thus it transmits negligible contractile forces to the calcaneus, and (b) the moment generated by all the other agonist and antagonist muscles that span the ankle joint is independent of knee angle. Both assumptions have previously been verified by EMG and direct moment measurements (Hof and van den Berg, 1977; Maganaris, 2001).

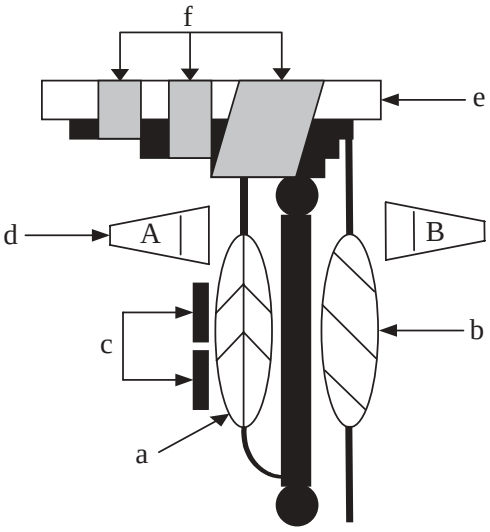

Fig. 1. The experimental set-up in our studies: (a) tibialis anterior (TA) muscle; (b) gastrocnemius (GS) muscle; (c) stimulating electrodes; (d) ultrasound probe, placed in position A for measurements in the TA tendon and in position B for measurements in the GS tendon; (e) dynamometer footplate; and (f) velcro straps. Ultrasound scanning was performed with the knee flexed at 90° for the TA tendon, and with the knee fully extended for the GS tendon.

Tendon elongations were obtained using a 7.5 MHz, B-mode, linear ultrasound probe (Esaote Biomedica, Florence, Italy; width and depth resolutions, 1 and 0.62 mm, respectively). First, consecutive axial-plane scans were taken along the belly of the in-series muscles to identify the borders of the muscle and the midpoint between them. A straight line was drawn through all midpoints marked along the muscle and assumed to be the midlongitudinal axis of the muscle–tendon unit. The scanning probe was displaced along this axis to locate the distal myotendinous junction of the muscle, over which it was fixed. The end point of the tendon in the myotendinous junction (the tendon origin) was the anatomical landmark whose position was traced to obtain tendon elongations during muscle contraction and subsequent relaxation. Muscle contraction−relaxa-relaxation cycles were then performed while, at the same time, video-recordings were made at 30 Hz of the sonographs taken. Echoabsorptive markers attached with an adhesive on the skin confirmed the absence of shifts in the scanning probe during contraction–relaxation.

To avoid artifactual elongations in the TA tendon due to a stretch in the retinaculum surrounding the tendon

(Maganaris et al., 1999), the ankle was bandaged with inelastic tape. For the GS tendon, additional ultrasound scans were taken over the calcaneus to measure the displacement of the tendon's bony attachment (the tendon insertion). The elongation of the tendon at any given load was then obtained by subtracting the displacement of the tendon insertion from the displacement of the tendon origin. The tendons' moment arm lengths were obtained from morphometric analysis of magnetic resonance images (General Electric, Signa Advantage 1.5 T/64 MHz, Milwaukee, USA), using the Reuleaux method for identifying the instantaneous centre of rotation in the tibiotalar joint (Rugg et al., 1990). The resting-state length of the tendons was measured manually to the nearest millimeter over the skin, following their path between origin and insertion. The cross-sectional area of the tendons was obtained from morphometric analysis of axial-plane sonographs.

Tendon forces were obtained by dividing the muscle moments recorded by the respective tendon moment arm lengths. Force–elongation relations during stretch (muscle contraction) and recoil (muscle relaxation) were obtained from load and displacement data corresponding to 0%, 20%, 40%, 60%, 80% and 100% of the maximal moment reached. Displacements were measured using computerized image analysis (NIH Image, Bethesdsa, USA). Force–elongation data were fitted with quadratic models. The tendon stiffness was calculated in the higher region of tendon force from the slope of the force–elongation curve. The tendon Young's modulus was calculated by multiplying the stiffness value obtained by the ratio of tendon length to tendon cross-sectional area. Mechanical hysteresis values were obtained from area calculations of the loop between the loading and unloading curves, using numerical integration.

Fig. 2 shows typical sonographs of the TA tendon origin during contraction–relaxation of the TA muscle. The TA tendon origin shifted proximally during contraction and distally during relaxation. The average value of maximal elongation obtained was 4.1 mm (2.5% strain). A similar behaviour was observed in the GS tendon origin, with the average value of maximal elongation obtained being 11.1 mm (4.9% strain). The tendon forces and stresses corresponding to the above elongations were 530 N and 25 MPa, respectively, in the TA tendon, and 875 N and 32 MPa, respectively, in the GS tendon. During muscle relaxation, the two tendons returned to their original positions following paths of larger displacement for any given load (Fig. 3). The quadratic models used for curve fitting yielded higher R^2 values than 0.98. The stiffness values obtained were 160 and 150 $N\,mm^{-1}$ for the TA and GS tendons, respectively, with the corresponding Young's modulus values being 1.2 and 1.16 GPa. The mechanical hysteresis values obtained were 19% and 18% for the TA and

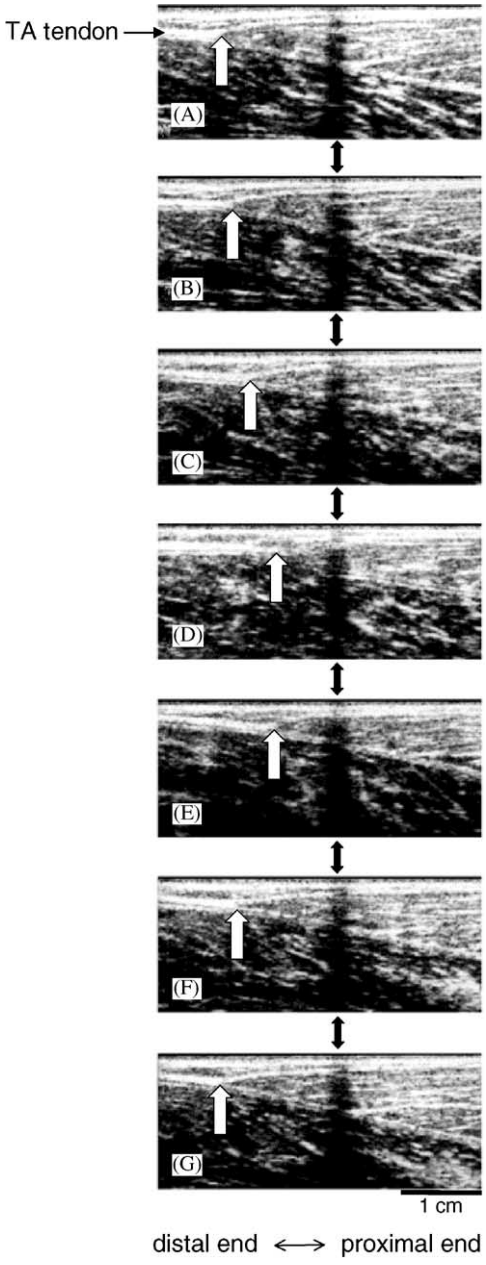

Fig. 2. Typical sonographs over the TA muscle–tendon unit: (A) original resting state; (B) 40% of M_{max} during contraction; (C) 80% of M_{max} during contraction; (D) 100% of M_{max} during contraction; (E) 80% of M_{max} during relaxation; (F) 40% of M_{max} during relaxation; and (G) 0% of M_{max} during relaxation. M_{max} is the maximal isometric moment of the TA muscle, produced by electrical stimulation. The white arrow in each scan points to the TA tendon origin. The black double arrows point to the shadow generated by an echoabsorptive marker glued on the skin to identify any displacements of the scanning probe during muscle contraction–relaxation. The tendon origin shifts proximally during contraction and distally during relaxation. The tendon origin displacement is larger during relaxation compared with contraction at each moment level, indicating the presence of mechanical hysteresis in the tendon. (From Maganaris and Paul, 2000a).

GS tendons, respectively. Inter- and intraobserver variations of the scanning procedures and image analyses involved were $<10\%$.

The curvilinear pattern of the force–elongation relations obtained indicate that the loads applied in either tendon lay within the "toe" region, i.e., were sufficient to align the collagen fibres in the tendon without causing further stretching. The TA tendon is designed for contractile force transmission to the bony attachment and it does not need to carry higher forces than those generated during maximal isometric contraction (Ker et al., 1988). Our results, therefore, suggest a limited chance of TA tendon failure by a single pull in real life, unless a sudden and forceful ankle plantarflexion occurs. The GS tendon, however, is designed for elastic energy storage–release and is called upon to withstand high forces generated during foot contact with the ground (Alexander, 1988; Ker et al., 1988). These forces may well exceed those obtained by maximal muscle contraction. In vivo measurements of tendon force indicate that the GS tendon may carry up to 110 MPa in each stride during running (Komi et al., 1992). This stress not only exceeds the estimated tendon stress of 15–30 MPa generated during maximal muscle contraction (Ker et al., 1988; Pike et al., 2000), but it also exceeds the average ultimate tensile stress of 100 MPa (Bennett et al., 1986), thus highlighting the possibility of GS tendon fracture in a single pull in real life. Epidemiological studies of spontaneous tendon rupture verify these theoretical considerations (Jozsa and Kannus, 1997).

The Young's modulus and maximal stress and strain values obtained in the above studies are similar to the respective values taken from excised tendons loaded with forces equivalent to the force-generating potential of the in-series muscles (Ker et al., 1988; Shadwick, 1990; Lieber et al., 1991). Similarly, the mechanical hysteresis values obtained fall within the range of values taken from isolated material (3–20%; Ker, 1981; Bennett et al., 1986; Pollock and Shadwick, 1994). In the TA tendon, the heat developed in each stretch–recoil cycle would not lead to hyperthermia, since the physiological loading of this tendon is low. In the GS tendon, however, generation of excessive heat is likely to occur due to the high, repeated tensile forces acting on this tendon during terrestrial locomotion. This could lead to thermal damage and predispose the tendon to mechanical failure. In fact, in vivo measurements and modelling-based calculations indicate that spring-like tendons may develop, during exercise, temperature levels above the 42.5°C threshold for fibroblast viability (Wilson and Goodship, 1994). These findings are in line with degenerative lesions often observed in the core of tendons acting as elastic energy stores, indicating that hyperthermia may be involved in the pathophysiology of exercise-induced tendon injuries.

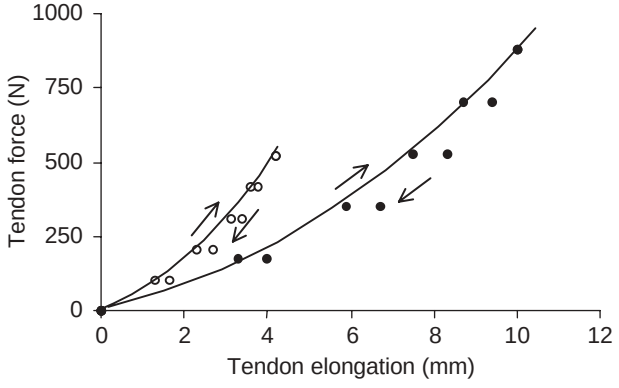

Fig. 3. Raw force–elongation data for the TA (open symbols) and GS (filled symbols) tendons in one subject. In each curve, arrows indicate loading and unloading directions. Data in the loading direction have been fitted with quadratic models.

Based on the adaptability of connective tissue to chronic use and disuse (Butler et al., 1978; Woo et al., 1980, 1982), it could be speculated that the GS tendon would be intrinsically stiffer than the TA tendon. Moreover, it could be speculated that the GS tendon would be more rebound resilient (rebound resilience = 1 − mechanical hysteresis) than the TA tendon, due to material adjustments for optimizing a spring-like behaviour (Shadwick, 1990). Our results, however, contrast these notions. The similarity of Young's modulus and mechanical hysteresis between the TA and GS tendons is in agreement with previous in vitro-based results showing an independence of tendon mechanical properties of anatomical site and physiological function (Pollock and Shadwick, 1994; Ker et al., 2000; Pike et al., 2000), thus suggesting that adjustments in tendon structural properties to physiological loading are accomplished by adding or removing material rather than altering the material's intrinsic properties.

In the second series of experiments, we investigated the hypotheses that: (a) the aponeurosis of a tendon elongates more than the tendon during contraction, and (b) the strain of the aponeurosis varies along its length.

To test the above hypothesis, we examined the TA tendon and its central aponeurosis (Maganaris and Paul, 2000b, c). We located three anatomical landmarks along the tendon-aponeurosis and we scanned by ultrasonography their displacements during isometric dorsiflexion contraction (Fig. 4). The first anatomical landmark was the TA tendon origin; its displacement upon contraction was obtained as described above and gave the elongation of the tendon (e_T). The second anatomical landmark was the proximal end of the TA central aponeurosis along the midlongitudinal axis of the muscle–tendon complex. Its displacement upon contraction gave the elongation of the tendon-aponeurosis (e_{T-A}), which was measured in a second series of contractions that generated the same moment with

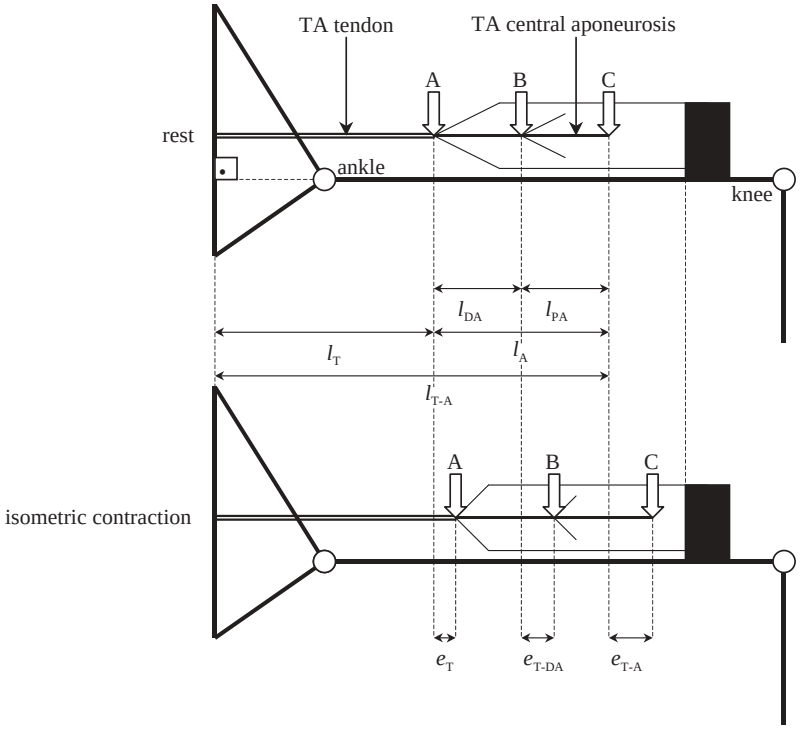

Fig. 4. Illustration of the method used to obtain elongations along the TA tendon-aponeurosis during contraction; (A) is the TA tendon origin; (B) is the intersection point between a central fascicle and the TA aponeurosis; and (C) is the proximal end of the TA aponeurosis. l_T is the tendon length, l_{T-A} is the tendon-aponeurosis length, l_A is the aponeurosis length, l_{DA} is the length of the aponeurotic distal region, and l_{PA} is the is the length of the aponeurotic proximal region. A, B and C shift proximally during isometric contraction of the TA muscle compared with rest. e_T is the elongation of the tendon, e_{T-A} is the elongation of the tendon-aponeurosis, and e_{T-DA} is the elongation of the tendon and aponeurotic distal region. The elongation of the aponeurosis (e_A) was estimated as $e_{T-A}-e_T$. The elongation of the aponeurotic proximal region (e_{PA}) was estimated as e_A-e_{DA} (from Maganaris and Paul, 2000c).

those used to obtain the e_T values. The elongation of the aponeurosis alone (e_A) was obtained as $e_{T-A}-e_T$. The third anatomical landmark was the intersection between a fascicle and the TA central aponeurosis. A fascicle in the midlength of the aponeurosis was scanned in all subjects in a third series of contractions that generated the same moments as those used to obtain the e_T and e_{T-A} values. The displacement of the fascicular insertion during contraction gave the elongation of the tendon and aponeurotic distal region (e_{T-DA}). The elongation of the aponeurotic distal region alone (e_{DA}) was obtained as $e_{T-DA}-e_T$. The elongation of the aponeurotic proximal region (e_{PA}) was obtained as e_A-e_{DA}. All elongations obtained were normalized to the initial lengths of the structures examined (measured over the skin) to obtain strain values.

Fig. 5 shows sonographs with the three anatomical landmarks identified. e_T and e_A increased curvilinearly until the load reached the maximal values of 4 mm (2.5% strain) and 12 mm (7% strain), respectively. e_{PA} and e_{DA} during isometric dorsiflexion MVC were 0.8 mm (9.2% strain) and 0.3 mm (3.5% strain), respectively (Fig. 6).

The strain values obtained in the above studies and the finding of a strain variation along the aponeurosis are in line with reports from experiments on isolated material (Huijing and Ettema, 1989; Ettema and Huijing, 1989; Lieber et al., 1991; Zuurbier et al., 1994; Loren and Lieber, 1995). Our results should not be interpreted as evidence that the tendon is structurally stiffer than the aponeurosis, and that the aponeurotic distal region is structurally stiffer than the aponeurotic proximal region. To draw conclusions about differences in structural stiffness, the same tensile force should act upon all structures, and this cannot be guaranteed with any protocol involving tendon-aponeurosis traction via muscle contraction. Although the tendon and the aponeurosis are placed in-series, they would be pulled by different forces, because different portions of the entire contractile material act upon them. According to the model shown in Fig. 4, the tendon is pulled by the contractile force elicited in the entire muscle, the aponeurotic distal end is pulled by almost half of the entire contractile force elicited, and the aponeurotic proximal end is pulled by the force elicited in the limited contractile material placed between the aponeurotic proximal end and the proximal end of the muscle–tendon complex. For homogeneous material properties along the tendon-aponeurosis, the above model would predict a smaller strain in the aponeurosis than the

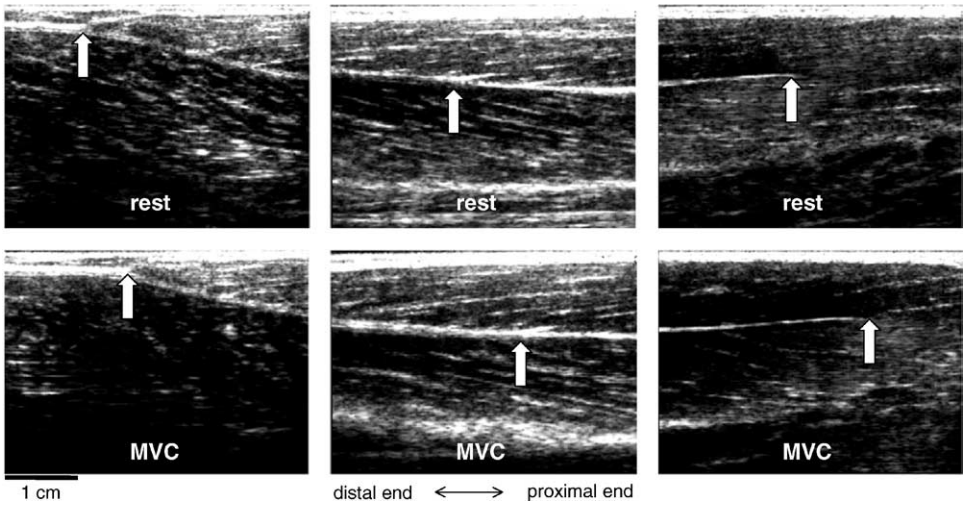

Fig. 5. Typical sonographs over the TA muscle–tendon unit at rest and during isometric dorsiflexion MVC. The arrows point to the reference points identified, i.e., the TA tendon origin (left), the intersection between a central fascicle and the central aponeurosis (middle), and the aponeurotic proximal end (right). All three reference points shift proximally during contraction (from Maganaris and Paul, 2000c).

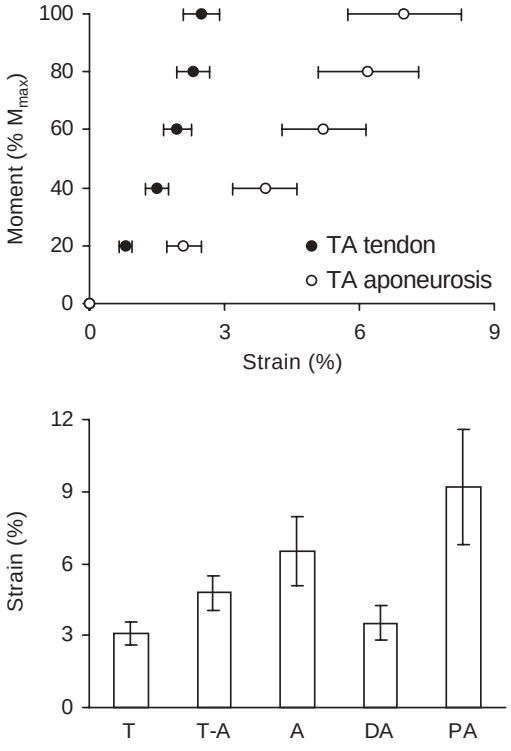

Fig. 6. Load–elongation relations in the TA tendon and its central aponeurosis (top), and strain distribution results along the entire TA tendinous component during isometric dorsiflexion MVC (bottom). M_{max} is the maximal isometric moment of the TA muscle, produced by electrical stimulation. T, tendon; T-A, tendon-aponeurosis; A, aponeurosis; DA, distal aponeurosis; PA, proximal aponeurosis. Values are means $\pm$SD. $N = 5$ for the graph at the top and $N = 6$ for the graph at the bottom (from Maganaris and Paul, 2000b, c).

tendon and a smaller strain in the aponeurotic distal end than the aponeurotic proximal end, which contrast the present findings. This could be attributed to differences in cross-sectional area along the tendon-aponeurosis. Anatomical observations on isolated specimens agree with this notion (Scott and Loeb, 1995).

The finding of a nonhomogeneous strain in the tendon-aponeurosis has important implications for muscle function. Muscle fibres attached to more extensible aponeurotic regions would shorten more upon contraction than fibres attached to less extensible aponeurotic regions. The extra shortening will result in shifting the force–length relation of the muscle–tendon unit to the right, which will result in a force enhancement in units operating in the descending limb of the force–length relation and in a force reduction in units operating in the ascending limb of the force–length relation (Zajac, 1989). In pennate structures, the extra shortening would bring about an increase in the pennation angle, and therefore a decrease in the effective vector of contractile force responsible for joint moment production. These considerations must be taken into account in muscle modelling applications.

The purpose of our third series of experiments was to investigate whether in vivo tendons exhibit loading history-dependent phenomena.

To test this hypothesis, we examined the GS tendons of six men. Scanning of the tendon origin in the myotendinous junction during isometric contractions was performed as described in the first series of our experiments. Five contractions were elicited 1 s apart, using tetanic (100 Hz), percutaneous electrical stimulation. For each subject, all contractions were elicited using the same voltage (the maximal tolerable voltage by the subject) and lasted 2 s. To establish the presence of creep in our test, the tendon elongation in all five contractions would need to correspond to the same joint moment; we decided to analyse elongations

corresponding to the joint moment generated in the fifth contraction, which yielded the lowest joint moment recorded in all five contractions in all subjects. All elongations obtained were corrected for the respective displacements in the tendon origin in the osteotendinous junction, assessed and analysed as described above.

The elongation of the tendon (expressed relative to the position of the tendon origin before the first contraction was elicited) increased in a curvilinear pattern, from 9.1 mm (4.7% strain) in the first contraction to 12 mm (6% strain) in the fifth contraction (Figs. 7 and 8).

The above findings agree with reports on the behaviour of excised tendon (for review see Viidik, 1973; Butler et al., 1978) and indicate that in vivo tendons may exhibit creep. These results have important biological implications for muscle–tendon units operating in an oscillating pattern in real life, clearly the GS, muscle–tendon unit is one of them. The creep induced in the tendon by the repeated loading would be taken up by the muscle fibres, which would then operate at shorter lengths. In vivo studies indicate that the GS muscle operates in the ascending limb of the force–length relation (Herzog et al., 1991), which indicates that tendon creep would reduce contractile force. Further reductions than those corresponding to sarcomeric force would be expected in the joint moment produced by contraction, due to increases in the pennation angle of the shortened fibres.

The creep in the tendon would result in shortening not only the extrafusal fibres but also the intrafusal fibres. This could trigger an alteration in proprioceptor firing

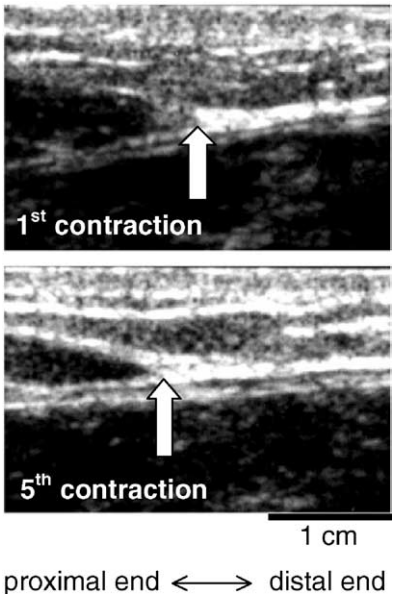

Fig. 7. Typical sonographs over the GS muscle–tendon unit in the first and fifth electrically stimulated contractions in one subject. The arrows point to the GS tendon origin. Both scans were taken at a plantarflexion moment of 82 Nm.

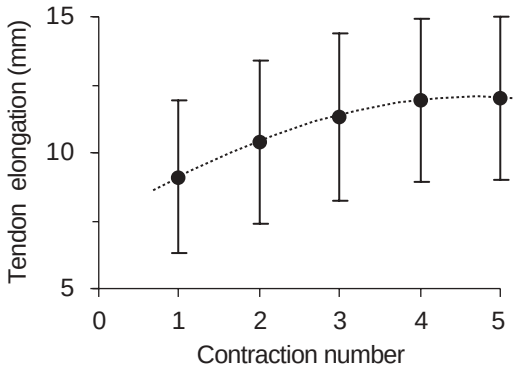

Fig. 8. Summarized results of GS tendon elongation in five consecutive electrically stimulated contractions producing a plantarflexion moment of 92 ± 11 Nm. The tendon length increases in a curvilinear fashion as a function of contraction number, indicating creep development in the tendon. Data are means $\pm$ SD ($N = 6$).

and erroneous feedback to the CNS with respect to the position of the limb. There are studies showing that changes in muscle length due to tendon extensibility are rather small to be seen by muscle spindles (Elek et al., 1990), but other experiments have challenged this view (Hoffer et al., 1989).

Finally, tendon creep might result in a fracture. Mathematical models based on results from experiments on excised specimens indicate that a tendon loaded by repeated cycles of maximal muscle contractions would fail in 4.2 h (Ker et al., 2000). For the GS tendon, which may be loaded with much higher loads physiologically (see Komi et al., 1992), the fatigue lifetime would be even smaller. This is an additional mechanism, which may be associated with the high incidence of injury in spring-like acting tendons.

2.1. Limitations of the method

Ultrasound-based assessment of the tensile properties of in vivo human tendon circumvents the limitations associated with testing isolated material. However, it does not avoid all problems:

(1) Heat loss from sources other than the tendon itself will be included in the measurements of tendon mechanical hysteresis. Extra heat dissipation (a) in the myotendinous and osteotendinous junctions, (b) in fatty structures in the sole of the foot, and (c) due to surface friction between the tendon and adjacent tissues, would be expected. This could explain the higher mechanical hysteresis values obtained with our protocol compared with the average value of $\sim 10\%$ obtained from measurements on isolated tendons (Ker, 1981; Pollock and Shadwick, 1994).

(2) The joint position that corresponds to 0% tendon strain and 0 N tendon force can only be assumed, unless a force transducer is inserted in the tendon (e.g. Komi et al., 1992; Finni et al., 1998). In our experiments, we

have chosen the neutral ankle position because it corresponded to minimal passive joint moments (see also Siegler et al., 1984). However, this could be the result of equal moments acting reciprocally around the ankle. Flexing or extending the ankle beyond its neutral position was not the preferred choice because we had no indication of the degree of slackness induced in each tendon.

(3) In the measurements of tendon elongation, the myotendinous junction is assumed to shift during contraction in the scanning plane only. However, a mediolateral displacement of the tendon might occur, especially in tendons acting through pulleys, resulting in erroneous elongations. 3-D ultrasound scanning could help eliminate such artifacts.

(4) The quantification of tendon load relies on the validity of 2-D procedures for estimating joint moments and tendon moment arm lengths. For the TA and GS tendons, the error introduced in the estimates of force would be rather small because the tibiotalar joint axis deviates by $<10^{\circ}$ from the position assumed in the measurements of moment and analyses of tendon moment arm length (Bogert van den et al., 1994). Moreover, the calculation of tendon force and stress in a given subject is based on the assumption that altering contractile force does not change the length of the tendon moment arm, despite in vivo experimental evidence showing that this assumption is in correct (Maganaris et al., 1998, 1999). Errors associated with inaccurate calculation of tensile loads would be eliminated with the use of transducers implanted in the tendon (e.g. Komi et al., 1992; Finni et al., 1998).

Additional problems will be encountered when deviating from the protocols described in our studies for quantifying tendon load and elongation. For example, several authors have failed to distribute the net moment generated during contraction to all agonist and antagonist muscles that cocontract upon activation (Kubo et al., 2001a, b; Magnusson et al., 2001; Muramatsu et al., 2001). In other experiments, the elongation of the tendon and part of the aponeurosis has been measured, and estimates of this structure's Young's modulus have been derived assuming that the tendon and the aponeurosis: (a) are pulled by similar forces (see the discussion in the second series of experiments described above), and (b) have the same structural properties (Kubo et al., 1999, 2000; Magnusson et al., 2001; Ito et al., 1998), despite experimental evidence of the opposite (Scott and Loeb, 1995). Such methodological problems can introduce substantial errors.

3. Applications of the method

The noninvasive nature of ultrasound allows design of longitudinal studies aimed at answering fundamental questions with clinical implications; for example, which training regime is most effective in enhancing the mechanical properties of a tendon? Or how long does it take before the mechanical properties of an immobilized tendon start to deteriorate? Moreover, our method can be of direct clinical use. Consider, for example, surgical procedures involving limb lengthening and tendon transfer. Any change in the resting-state length of the tendon will alter its extensibility and this will clearly affect the function of the in-series muscle. In this direction, protocols for assessing the tendon mechanical properties in the in vivo state could provide crucial help for optimizing the outcome of a corrective surgery; for example, they could be used for measurements in the tendon of the contralateral healthy limb of a patient, thus providing reference values that could then be used for guiding the surgical decision making.

References

Alexander, R.McN., 1988. Elastic Mechanisms in Animal Movement. Cambridge University Press, Cambridge.

Bennett, M.B., Ker, R.F., Dimery, N.J., Alexander, R.McN., 1986. Mechanical properties of various mammalian tendons. Journal of Zoology London (A) 209, 537–548.

Bogert van den, A.J., Smith, G.D., Nigg, B.M., 1994. In vivo determination of the anatomical axes of the ankle joint complex: an optimization approach. Journal of Biomechanics 27, 1477–1488.

Bottinelli, R., Canepari, M., Pellegrino, M.A., Reggiani, C., 1996. Force–velocity properties of human skeletal muscle fibres: myosin heavy chain and temperature dependence. Journal of Physiology 495, 573–586.

Butler, D.L., Goods, E.S., Noyes, F.R., Zernicke, R.F., 1978. Biomechanics of ligaments and tendons. Exercise Sports Sciences Reviews 6, 125–181.

Elek, J., Prochazka, A., Hulliger, M., Vincent, S., 1990. In-series compliance of gastrocnemius muscle in cat step cycle: do spindles signal origin-to-insertion length? Journal of Physiology 429, 237–258.

Ettema, G.J.C., Huijing, P.A., 1989. Properties of the tendinous structures and series elastic component of the EDL muscle–tendon complex of the rat. Journal of Biomechanics 22, 1209–1215.

Finni, T., Komi, P.V., Lukkariniemi, J., 1998. Achilles tendon loading during walking: application of a novel optic fiber technique. European Journal of Applied Physiology 77, 289–291.

Herzog, W., Read, L.J., ter Keurs, H.E.D.J., 1991. Experimental determination of force–length relations of intact human gastrocnemius muscles. Clinical Biomechanics 6, 230–238.

Hof, A.L., van den Berg, J.W., 1977. Linearity between the weighted sum of the EMGs of the human triceps surae and the total torque. Journal of Biomechanics 10, 529–539.

Hoffer, J.A., Caputi, A.A., Pose, I.E., Griffiths, R.I., 1989. Roles of muscle activity and load on the relationship between muscle spindle length and whole muscle length in the freely walking cat. Progress in Brain Research 80, 75–85.

Huijing, P.A., Ettema, G.J.C., 1988/1989. Length–force characteristics of aponeurosis in passive muscle and during isometric and slow dynamic contractions of rat gastrocnemius muscle. Acta Morphologica Neerlando-Scandinavica 26, 51–62.

Ito, M., Kawakami, Y., Ichinose, Y., Fukashiro, S., Fukunaga, T., 1998. Nonisometric behaviour of fascicles during isometric

contractions of human muscle. Journal of Applied Physiology 85, 1230–1235.
Jozsa, L.G., Kannus, P., 1997. Spontaneous rupture of tendons. In: Jozsa, L.G., Kannus, P. (Eds.), Human Tendons: Anatomy, Physiology and Pathology. Human Kinetics, Champaign, pp. 254–325.
Ker, R.F., 1981. Dynamic tensile properties of the plantaris tendon of sheep (*Ovies aries*). Journal of Experimental Biology 93, 283–302.
Ker, R.F., 1992. Tensile fibres: strings and straps. In: Vincent, J.F.V. (Ed.), Biomechanics—Materials: A Practical Approach. Oxford University Press, New York, pp. 75–97.
Ker, R.F., Alexander, R.McN., Bennett, M.B., 1988. Why are mammalian tendons so thick? Journal of Zoology London 216, 309–324.
Ker, R.F., Wang, X.T., Pike, A.V.L., 2000. Fatigue quality of mammalian tendons. Journal of Experimental. Biology 203, 1317–1327.
Komi, P.V., Fukashiro, S., Jarvinen, M., 1992. Biomechanical loading of Achilles tendon during normal locomotion. Clinical Sports Medicine 11, 521–531.
Kubo, K., Kawakami, Y., Fukunaga, T., 1999. The influence of elastic properties of tendon structures on jump performance in humans. Journal of Applied Physiology 87, 2090–2096.
Kubo, K., Kanehisa, H., Kawakami, Y., Fukunaga, T., 2000. Influence of static stretching on viscoelastic properties of human tendon structures in vivo. Journal of Applied Physiology 90, 520–527.
Kubo, K., Kanehisa, H., Kawakami, Y., Fukunaga, T., 2001a. Influences of repetitive muscle contractions with different modes on tendon elasticity in vivo. Journal of Applied Physiology 91, 277–282.
Kubo, K., Kanehisa, H., Kawakami, Y., Fukunaga, T., 2001b. Growth changes in the elastic properties of human tendon structures. International Journal of Sports Medicine 22, 138–143.
Lieber, R.L., Leonard, M.E., Brown, C.C., Trestic, C.L., 1991. Frog semitendinosis tendon load–strain and stress–strain properties during passive loading. American Jounal of Physiology 30, C86–C92.
Loren, G.J., Lieber, R.L., 1995. Tendon biomechanical properties enhance human wrist muscle specialization. Journal of Biomechanics 28, 791–799.
Maganaris, C.N., 2001. Force–length characteristics of in vivo human skeletal muscle. Acta Physiologica Scandinavica 172, 279–285.
Maganaris, C.N., Paul, J.P., 1999. In vivo human tendon mechanical properties. Journal of Applied Physiology 521, 307–313.
Maganaris, C.N., Paul, J.P., 2000a. Hysteresis measurements in intact human tendon. Journal of Biomechanics 33, 1723–1727.
Maganaris, C.N., Paul, J.P., 2000b. Load–elongation characteristics of in vivo human tendon and aponeurosis. Journal of Experimental Biology 203, 751–756.
Maganaris, C.N., Paul, J.P., 2000c. In vivo human tendinous tissue stretch upon maximal muscle force generation. Journal of Biomechanics 33, 1453–1459.
Maganaris, C.N., Paul, J.P., 2002. Tensile properties of the in vivo human gastrocnemius tendon. Journal of Experimental Biology, in preparation.
Maganaris, C.N., Baltzopoulos, V., Sargeant, A.J., 1998. Changes in Achilles tendon moment arm from rest to maximum isometric plantarflexion: in vivo observations in man. Journal of Physiology 510, 977–985.
Maganaris, C.N., Baltzopoulos, V., Sargeant, A.J., 1999. Changes in the tibialis anterior moment arm from rest to maximum isometric dorsiflexion: in vivo observations in man. Clinical Biomechanics 14, 661–666.
Magnusson, S.P., Aagaard, P., Rosager, S., Dyhre-Poulen, P., Kjaer, M., 2001. Load–displacement properties of the human triceps surae aponeurosis in vivo. Journal of Physiology 531, 277–288.
Matthews, L.S., Ellis, D., 1968. Viscoelastic properties of cat tendon: effects of time after death and preservation by freezing. Journal of Biomechanics 1, 65–71.
Muramatsu, T., Muraoka, T., Takeshita, D., Kawakami, Y., Hirano, Y., Fukunaga, T., 2001. Mechanical properties of tendon and aponeurosis of human gastrocnemius muscle in vivo. Journal of Applied Physiology 90, 1671–1678.
Pike, A.V.L., Ker, R.F., Alexander, R.McN., 2000. The development of fatigue quality in high- and low-stressed tendons of sheep (*Ovis aries*). Journal of Experimental Biology 203, 2187–2193.
Pollock, C.M., Shadwick, R.E., 1994. Relationship between body mass and biomechanical properties of limb tendons in adult mammals. American Journal of Physiology 266, R1016–R1021.
Powell, P.L., Roy, R.R., Kanim, P., Bello, M.A., Edgerton, V.R., 1984. Predictability of skeletal; muscle tension from architectural determinations in guinea pig hindlimbs. Journal of Applied Physiology 57, 1715–1721.
Rugg, S.G., Gregor, R.J., Mandelbaum, B.R., Chiu, L., 1990. In vivo moment arm calculations at the ankle using magnetic resonance imaging (MRI). Journal of Biomechanics 23, 495–501.
Scott, S.H., Loeb, G.E., 1995. Mechanical properties of aponeurosis and tendon of the cat soleus muscle during whole-muscle isometric contractions. Journal of Morphology 224, 73–86.
Shadwick, R.E., 1990. Elastic energy storage in tendons: mechanical differences related to function and age. Journal of Applied Physiology 68, 1033–1040.
Shadwick, R.E., 1992. Soft composites. In: Vincent, J.F.V. (Ed.), Biomechanics—Materials: A Practical Approach. Oxford University Press, New York, pp. 133–164.
Siegler, S., Moskowitz, G.D., Freedman, W., 1984. Passive and active components of the internal moment developed about the ankle joint during ambulation. Journal of Biomechanics 19, 647–652.
Smith, C.W., Young, I.S., Kearney, J.N., 1996. Mechanical properties of tendons: changes with sterilization and preservation. Journal of Biomechanical Engineering 118, 56–61.
Viidik, A., 1973. Functional properties of collagenous tissues. International Review of Connective Tissue Research 6, 127–215.
Wilson, A.M., Goodship, A.E., 1994. Exercise-induced hyperthermia as a possible mechanism for tendon degeneration. Journal of Biomechanics 27, 899–905.
Witzmann, F.A., Kim, D.H., Fitts, R.H., 1983. Effect of hindlimb immobilization on the fatigability of skeletal muscle. Journal of Applied Physiology 54, 1242–1248.
Woo, S.L.-Y., Ritter, M.A., Amiel, D., Sanders, T.M., Gomez, M.A., Kuei, S.C., Garfin, S.R., Akeson, W.H., 1980. The biomechanical and biochemical properties of swine tendons—long term effects of exercise on the digital extensors. Connective Tissue Research 7, 177–183.
Woo, S.L.-Y., Gomez, M.A., Woo, Y.-K., Akeson, W.H., 1982. Mechanical properties of tendons and ligaments II. The relationships of immobilization and exercise on tissue remodelling. Biorheology 19, 397–408.
Zajac, F.E., 1989. Muscle and tendon: properties, models, scaling, and application to biomechanics and motor control. CRC Critical Reviews of Biomedical Engineering 17, 359–411.
Zernicke, R.F., Butler, D.L., Grood, E.S., Hefzy, M.S., 1984. Strain topography of human tendon and fascia. Journal of Biomechanical Engineering 106, 177–180.
Zuurbier, C.J., Everard, A.J., van der Wees, P., Huijing, P.A., 1994. Length–force characteristics in the passive and active muscle conditions and in the isolated condition. Journal of Biomechanics 27, 445–453.